Surface Proton Donors for the D-Pathway of Cytochrome *c* Oxidase in the Absence of Subunit III[†]

Pia Ädelroth*,[‡] and Jonathan Hosler*,[#]

Department of Biochemistry and Biophysics, The Arrhenius Laboratories for Natural Sciences, Stockholm University, SE-106 91 Stockholm, Sweden, and Department of Biochemistry, University of Mississippi Medical Center, 2500 North State Street, Jackson, Mississippi 39216

Received March 24, 2006; Revised Manuscript Received May 10, 2006

ABSTRACT: The major proton-transfer pathway into the buried active site of cytochrome *c* oxidase (C*c*O) is the D-pathway that begins with the subunit I residue Asp-132 on the inner protein surface (the cytoplasmic surface of the aa_3-type C*c*O of *Rhodobacter sphaeroides*). Asp-132 is surrounded by residues from both subunits I and III. In the absence of subunit III, C*c*O retains activity, but the functional characteristics of the D-pathway are significantly altered such that the transfer of protons from Asp-132 into the pathway becomes the rate-limiting step. Determination of the pH-dependence of the rate constant for D-pathway proton uptake during the single-turnover of C*c*O indicates that the pK_a of Asp-132 in the absence of subunit III is ∼7. The removal of subunit III also allows for alternative surface proton donor/acceptors other than Asp-132. With Asp-132 altered to alanine, the rate constant for D-pathway proton uptake is very slow (5 s^{-1}) in the presence of subunit III. Once subunit III is removed, the proton uptake rate constant increases 80-fold, to 400 s^{-1}. The pK_a associated with this uptake is >10, and the initial proton donor/acceptor in D132A III (−) is proposed to be a water of the D-pathway rather than an amino acid residue. Arachidonic acid (Aa), which stimulates the activity of several D-pathway mutant C*c*Os, appears to become the initial proton donor/acceptor in the absence of subunit III, whether or not Asp-132 is altered. Aa shifts the pK_a of the initial proton donor to 7.6 for both wild-type (WT) III (−) and D132A III (−). The results indicate that subunit III creates a barrier that helps prevent protons from donors other than Asp-132 from directly accessing the internal waters of the D-pathway, while the subunit also provides an environment that increases the rate at which Asp-132 transfers protons into the D-pathway.

Cytochrome *c* oxidase (C*c*O)[1] is the last complex in the aerobic respiratory chain of mitochondria and many bacteria. It uses electrons from a water-soluble cytochrome (cyt) *c* to reduce molecular oxygen to water. During this process, the protons needed for water formation are taken from the negative (inside) N-side, i.e., the matrix in mitochondria or the cytoplasm in bacteria. In addition, for every electron transferred from cyt *c* to O_2, one proton is translocated, pumped, through the protein and released on the positive (outside) P-side (eq 1). C*c*O thereby contributes to the transmembrane proton electrochemical gradient, which is used by the organism for energy-requiring processes (for reviews on C*c*O structure and function, see e.g., refs *1*−*4*).

$$O_2 + 8H^+_{in} + 4e^- \rightarrow 2H_2O + 4H^+_{out} \qquad (1)$$

C*c*Os belong to a superfamily of oxidases characterized by a central catalytic subunit (subunit I), generally containing 12 transmembrane helices, that bind a low-spin heme which transfers electrons to a binuclear metal center, composed of a high-spin heme and a copper ion, where oxygen is reduced to water (*5*). C*c*O from *Rhodobacter sphaeroides* is composed of four subunits (see Figure 1A). Subunit I harbors the heme a_3−Cu_B active site and low-spin heme *a*, while subunit II is a membrane-anchored protein with a globular periplasmic domain containing the dicopper center, Cu_A, the site of electron entry from water-soluble cyt *c*. Subunit III is a highly hydrophobic peptide composed of seven transmembrane helices; subunit III binds to subunit I opposite the two transmembrane helices of subunit II. Subunit III does not contain a redox center, and it is not required for the assembly of any of the redox centers in subunits I and II (*6*). In its absence, however, C*c*O inactivates with turnover, such that at pH 7.5 its catalytic lifetime is less than 0.1% that of the normal oxidase containing subunit III (*7*, *8*). Subunit IV is a one-helix peptide with unknown function.

The heme a_3−Cu_B oxygen reduction site in C*c*O is buried in the membrane-spanning region of subunit I, ∼30 Å from the cytoplasmic surface. Two proton pathways, identified by structural and functional analyses, lead from the inner surface of the protein to the active site, the D- and K-pathways (see Figure 1B).

The K-pathway, which gets its name from a conserved, functionally important lysine, Lys-362 (*R. sphaeroides*

[†] These studies were supported by Grant NIH GM56824 to J.H. and by a grant from the Swedish Research Council to P.Ä.

* Corresponding authors: (P.Ä.) E-mail: piaa@dbb.su.se; phone: +46-8-164183; fax: +46-8-153679, and (J.H.) E-mail: jhosler@biochem.umsmed.edu; phone: +1-601-984-1861; fax: +1-601-984-1501.

[‡] Stockholm University.

[#] University of Mississippi Medical Center.

[1] Abbreviations: C*c*O, cytochrome *c* oxidase; DDM, β-D-dodecyl maltoside; PMS, phenazine methosulfate; Aa, arachidonic acid; WT, wild-type C*c*O; WT III (−), wild-type C*c*O lacking subunit III.

10.1021/bi0605843 CCC: $33.50
Published on Web 06/15/2006

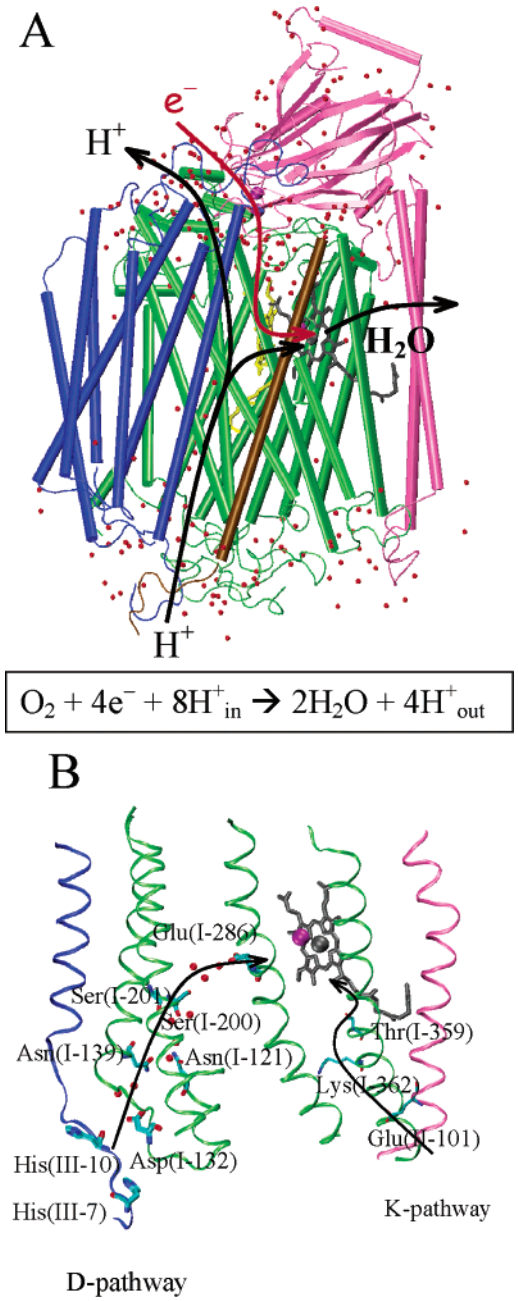

FIGURE 1: (A) The structure of C*c*O from *R. sphaeroides* (coordinates from pdb ID 1M56 (*35*)). Subunits I, II, III, and IV are indicated in green, pink, blue, and brown, respectively. Also shown are water molecules resolved in the structure (red spheres) and the heme groups in yellow (heme *a*) and dark gray (heme a_3). The pictures were made using the VMD software (*40*). (B) Part of the structure around the catalytic site (heme a_3 and Cu_B in dark gray and magenta, respectively) of C*c*O, emphasizing the D-pathway for proton transfer with some of the crystallographically resolved water molecules. Also shown is the K-pathway. For details, see text.

numbering and, unless otherwise indicated, the residues are in subunit I), is used during the reductive phase of the catalytic cycle for the uptake of one or two protons. The D-pathway, named for Asp-132 at the surface of the protein, transfers protons to the heme a_3−Cu_B site after oxygen is bound, plus all of the protons destined to be pumped. The D-pathway extends from Asp-132 on the surface of the protein, through one (possibly two) waters to a pair of asparagine residues, Asn-121 and Asn-139, and then through a longer series of waters to Glu-286, some 26 Å above Asp-132 and ~10 Å from the active site. Another series of waters, modeled but unresolved in structures, takes the protons from Glu-286 to the active site. Asp-132 is located at a junction between subunits I and III on the inner surface of the oxidase, in a shallow well. The maximum rate of proton transfer through the normal D-pathway is fast, greater than 10^4 s^{-1}.

A powerful tool for investigating the mechanism of O_2 reduction and proton uptake through the D-pathway by C*c*O is the so-called "flow-flash technique". In this technique, carbon monoxide (CO) is bound to the active site heme of the fully reduced C*c*O, the CO-bound oxidase is mixed with oxygenated buffer, and the reaction with O_2 is initiated by a laser flash that breaks the photolabile heme a_3−CO bond and allows O_2 to bind and be reduced. In the aa_3-type C*c*O of *R. sphaeroides*, the sequence of events and their corresponding time constants are as follows (*9*) (see Figure 2 for a summary of the transitions in the reaction). Oxygen binds to form the Fe^{2+}-O_2 intermediate termed A (τ_{R-A}~ 10 μs). In a rapid rearrangement, four electrons are transferred to the bound O_2, one from Cu_B, two from heme a_3, and one from heme *a*. This rearrangement breaks the O−O bond and forms intermediate P^3 (the superscript indicates the number of electrons transferred from an external donor into the binuclear site up to this point) (τ_{A-P} ~ 40 μs), composed of an oxyferryl on heme a_3 ($a_3{}^{4+}$ = O) and a hydroxyl group on Cu_B ($Cu_B{}^{2+}$-OH^-). Formation of the P^3 intermediate also requires a proton provided internally, presumably from Tyr-288 (*10*, *11*). Rapid transfer of a proton from Glu-286 to the deprotonated Tyr (or the hydroxyl group on Cu_B) forms the F^3 oxoferryl intermediate (τ_{P-F} ~ 100 μs); Glu-286 is rapidly reprotonated by the transfer of a proton from the bulk solution through the D-pathway, observed with the same time constant (100 μs). The final step is the slower conversion of F^3 to the $O^{4/0}$ (oxidized) intermediate (τ_{F-O} ~ 1.2 ms). This step involves simultaneous electron transfer from the Cu_A/heme *a* equilibrium and proton transfer through the D-pathway to create [Fe^{3+}-OH^- $Cu_B{}^{2+}$-OH^-]. Thus, two protons are taken up through the D-pathway in the single-turnover experiment, one during the $P^3 \rightarrow F^3$ transition and one during the slower $F^3 \rightarrow O^{4/0}$ transition (hereafter referred to as P → F and F → O).

Subunit III is needed to maintain rapid proton uptake through the D-pathway at physiologic pH (*12*). At pH 7.5, without subunit III, no protons are taken up on the time-scale of the P → F transition during the single-turnover experiment. Rather, both protons are taken up during the F → O transition (τ_{F-O} in WT III (−) ~ 2 ms), which makes the maximum proton uptake rate at least 20-fold slower than in WT C*c*O containing subunit III at pH 7.5 (*12*). It was speculated that the retardation of proton uptake in the absence of subunit III may be due to disruption of the "proton-collecting antenna" of C*c*O and/or to greater stabilization of the anionic form of Asp-132 (a decline in its pK_a) as the residue becomes more exposed to bulk water (*12*). Rapid proton uptake is restored to WT III (−) at low pH, and the observed pK_a in the F → O transition is lowered by about two pH units (*12*).

More recently, it has been shown that slow proton uptake through the D-pathway increases the probability of turnover-dependent suicide inactivation at the active site of C*c*O,

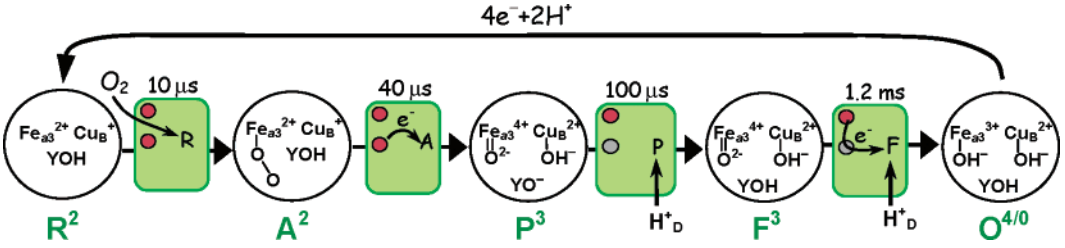

FIGURE 2: Simplified catalytic cycle indicating the sequence of electron and proton transfers in the flow-flash reaction between fully reduced WT C*c*O from *R. sphaeroides* and O_2 (*9*). Also indicated are the structures of the oxygen intermediates at the catalytic site, where YOH represents the Tyr-288. The superscript indicates the number of electrons transferred from the external donor to the binuclear site. Filled red circles indicate reduced Cu_A (top) and heme *a*. The reaction starts after flash-induced dissociation of CO from the fully reduced C*c*O. O_2 binds with $\tau = 10$ μs (at 1 mM O_2), after which the P^3 intermediate is formed ($\tau = 40$ μs) by electron transfer from heme *a* to the binuclear site. The F^3 intermediate is then formed ($\tau = 100$ μs) by uptake of a proton through the D-pathway. Concomitantly with the P → F transition, there is a fractional electron transfer from Cu_A to heme *a* (not shown). The last step is the formation of the oxidized, O intermediate ($\tau = 1.2$ ms) by electron transfer from the Cu_A/heme *a* equilibrium and proton uptake through the D-pathway.

presumably due to destructive chemistry that results from the increased lifetimes of the reactive oxoferryl intermediates during the catalytic cycle (*8*). This is consistent with the increased probability of suicide inactivation in the absence of subunit III since proton uptake through the D-pathway is slower without subunit III. A practical consequence of this finding is that measurements of the catalytic life span of mutant C*c*O forms, in terms of the number of catalytic cycles performed before inactivation, can be used as an indirect measure of the efficiency of proton uptake by the D-pathway during steady-state O_2 reduction.

Somewhat surprisingly, in the D132A mutant C*c*O, where turnover activity is only 2−3% of that in the WT (*13*, *14*), the effect of removing subunit III is a *stimulation* of turnover activity to about 40% of that of WT III (−) (*15*). The initial proton donor/acceptor that substitutes for Asp-132 in the absence of subunit III has been speculated to be His-26, a close neighbor of Asp-132 (*15*) (see Figure 8). In this study, we have utilized two independent techniques, time-resolved single-turnover flow-flash studies of electron and proton-transfer plus measurements of catalytic life span during steady-state O_2 reduction, to investigate the dynamics and pH dependence of proton transfer through the D-pathway in D132A III (−) and WT III (−). The obtained data for the F → O transition of WT III (−) and D132A III (−) leads to the conclusion that the pK_a of Asp-132 in the absence of subunit III is 7. For D132A, the results show an 80-fold increase in the rate of proton uptake upon the removal of subunit III, thus explaining the increased O_2 reduction activity of D132A III (−) (*15*). In addition, it is shown that the initial donor that takes over the role of the Asp-132 in the absence of subunit III and Asp-132 has a much higher pK_a than Asp-132 and is likely to be a water of the D-pathway. Furthermore, arachidonic acid (Aa), which stimulates activity in several D-pathway mutant C*c*Os, can take over the role as initial proton donor, shifting the pH dependence back into the physiological range and making the proton-transfer characteristics of WT III (−) and D132A III (−) essentially identical.

MATERIALS AND METHODS

Enzyme Purification and Steady-State Catalytic Activity Measurements. Bacterial growth, oxidase purification, and the removal of subunit III were performed as in Zhen et al. (*16*) and Mills et al. (*15*).

The measurements of catalytic life span as the CC_{50}, including data evaluation, were performed as in Mills and Hosler (*8*). The CC_{50} is the average catalytic life span of the C*c*O form, in terms of catalytic cycles (not time), where one catalytic cycle is defined as $1O_2 \rightarrow 2H_2O$. For the pH-dependence measurements, pH values between 6.2 and 6.8 were obtained using 50 mM MES−KOH, from 6.8 to 8.2 using 50 mM HEPES−KOH and from 8.2 to 9.0 using CHES−KOH. The buffer at each pH was adjusted to 50 mM ionic strength using KCl. The lines through each data set (with the exception of those showing no pH dependence) are nonlinear regression curves generated by a sigmoidal function using the equation $CC_{50} = CC_{50min} + (CC_{50max} - CC_{50min})/(1 + 10^{((pH-pK_a)*slope)})$.

Construction of H26A−D132A. Beginning with a 2.1 kbp *Hin*d III fragment (in pUC19) containing *coxI* (the gene for subunit I) with the D132A mutation (obtained from C. Hiser and S. Ferguson-Miller, Michigan State University), QuikChange mutagenesis (Qiagen) was used to insert a sequence coding for SNHHHHHH immediately prior to the stop codon at the C-terminus of *cox I*. The H26A mutation was then introduced by QuikChange. The mutated *coxI* was cloned into the *Hin*d III site of a pRK415-based plasmid (*17*), pLH449, which contains a truncated *coxII−III* operon composed of *coxII* (the gene for subunit II), cox10 (heme O synthase), and cox11 (Cu_B insertion) (*18*, *19*). The resulting plasmid, pLH449/H26A-D132A I-his, was conjugated into the *R. sphaeroides* strain JS100, which lacks the WT gene for subunit I (*20*). The JS100 strain also contained the pBBR1MCS-2-based (*21*) plasmid pJG211 from a previous conjugation. pJG211 expresses subunit III under the direction of the *coxI* promoter; details of its construction will be published elsewhere. Thus, the completed *R. sphaeroides* strain expresses H26A−D132A subunit I, with a C-terminal six-histidine tag, and WT subunit II from one plasmid (pLH449/H26A−D132A I-his), and WT subunit III from a different but compatible plasmid (pJG211).

Flow-Flash Experiments. C*c*O samples for flow-flash measurements were prepared essentially as in ref *9*. Briefly, the enzyme was diluted to ~10 μM in 100 mM Hepes-KOH (pH 7.4), 0.05% (w/v) β-dodecyl-maltoside (DDM) except for the pH-dependence measurements, in which the diluted C*c*O stock contained only 5 mM Hepes. The C*c*O solution was transferred to a modified anaerobic cuvette, and the electron mediator phenazine methosulfate (PMS) was added to 0.2 μM. After the air was exchanged for nitrogen on a

vacuum line, the enzyme was reduced by the anaerobic addition of 2 mM ascorbate, after which N_2 was exchanged for CO.

Flow-flash measurements were performed using the apparatus described in ref *22*. Briefly, fully reduced CO-bound C*c*O was mixed 1:5 with an oxygenated buffer in a modified stopped-flow apparatus (Applied Photophysics, UK). After 200 ms, a 10 ns laser flash (Nd:YAG laser, Quantel) was applied, dissociating CO and allowing O_2 to bind and initiate electron transfer. The time course of the reaction was studied from microseconds to seconds at different wavelengths. Typically, at each wavelength, 3×10^4 data points were collected, and the data set was then reduced to 1000 points by averaging over a progressively increasing number of points (logarithmic time scale). For the pH-dependence measurements, the oxygenated solution contained 100 mM of either citrate (pH 5.0−6.0), Mes (pH 6.0−7.0), Hepes (pH 7.0−8.0), Tris (pH 8.0−9.0), or Caps (pH 9.0−10.0) depending on the final pH required. For measurements with Aa, the final concentration of Aa was achieved by adding it to both the C*c*O sample and the oxygenated-buffer from a stock of 50 mM Aa prepared in ethanol.

Proton-Uptake Measurements. The kinetics of proton uptake during O_2 reduction were measured at pH ~7.5 essentially as in ref *9*. Briefly, the buffer in the C*c*O solution was exchanged for 50 mM KCl, 0.05% DDM on a PD-10 column (Pharmacia), and the pH was adjusted to ~7.5. The pH sensitive dye phenol red was added to a final concentration of 40 μM. After the fully reduced CO-bound C*c*O was prepared as above, the pH was readjusted to ~7.5, as judged by the absorbance of the dye. In the flow-flash reaction, the oxygen-saturated buffer-free solution contained 50 mM KCl, 0.05% DDM, and 40 μM phenol red, at pH ~7.5. To correct for the residual contribution from the redox reactions to the observed signal at 560 nm (the absorbance maximum of the dye), traces were also collected in the presence of buffer. The trace obtained in the presence of buffer was then subtracted from that obtained in the absence of buffer.

Data Handling and Analysis. To extract the rate constants of the observed phases in the flow-flash reaction, the time-resolved changes in absorbance, measured at different wavelengths, were fitted either separately or globally to a model of consecutive irreversible reactions (e.g., A → B → C) using the software package Pro-K (Applied Photophysics, UK). The pH-dependencies of the rate constants for the F → O transition in the different C*c*Os were fitted to a simple Henderson−Hasselbalch titration of one protonatable group using the equation $k_{obs(F-O)} = k_{min(F-O)} + (k_{max(F-O)} - k_{min(F-O)})/(1 + 10^{pH-pK_a})$.

RESULTS

Single Turnover Oxygen Reduction and Proton Uptake by D132A in the Presence and Absence of Subunit III. Mutation of Asp-132, the initial proton acceptor/donor of the D-pathway, to alanine, slows the rate of steady-state O_2 reduction from ~2000 to ~30 e^- s^{-1} (*13*, *15*). Where in the catalytic cycle this inhibition occurs in the mutant C*c*O is evident from studies of the single turnover reaction of the fully reduced enzyme with oxygen, presented in Figure 3A,B. After CO dissociation, formation of the A and P^3 intermediates is clearly seen at 445 nm, where hemes *a* and a_3 absorb. These intermediates are formed in D132A with the same rate constants as in the WT enzyme (see Figure 2 for a summary of the reactions involved in the different steps). The F intermediate is also formed with the normal rate constant in D132A, which was more clearly seen at 580 nm, the absorbance peak in the difference spectrum F minus O (data not shown). However, conversion of the F intermediate to form the fully oxidized intermediate, O, is severely inhibited in D132A, to ~5 s^{-1} (see Figure 3A,B) as compared to ~800 s^{-1} in WT. For WT C*c*O, the uptake of ~1 H^+ from the bulk solution, measured using the pH-sensitive dye phenol red, occurs simultaneously with the P → F transition ($k_{P-F} \sim 10^4$ s^{-1}) and ~1 H^+ is taken up during the F → O transition ($k_{F-O} \sim 800$ s^{-1}) (for a detailed explanation of proton uptake rates and stoichiometry, see ref *9*). In D132A, however, there is no proton uptake on the P → F time-scale. Instead, two protons are taken up during the slow F → O transition (5 s^{-1}) (Figure 3B). This means that the proton used to form intermediate F is provided internally, presumably from Glu-286 (see ref *23* and Discussion). Thus, the ultimate fate of the two protons taken up by D132A is presumably the same as in WT; one is used to reprotonate Glu-286, while the other protonates the oxoferryl intermediate in the conversion of F to O. However, the rate of proton uptake through the D-pathway is inhibited over 3 orders of magnitude (5 s^{-1} compared to 10^4 s^{-1}) by the alteration of Asp-132 to a non-carboxylate residue. The observed slow proton uptake in D132A may actually not take place through the D-pathway at all, since experimental evidence indicates that the slow rate of O_2 reduction by D132A is supported by proton flow from the outer surface of C*c*O to the active site (*24*, *25*).

When subunit III is removed from D132A, its rate of steady-state O_2 reduction *increases* substantially to ~400 e^- s^{-1} at pH 7.4 (*15*). As seen in Figure 3C,D, the increased activity of D132A III (−) is due to an 80-fold increase in the rate of proton uptake through the D-pathway, giving a rate constant for the F → O transition of ~400 s^{-1} (at pH 7.4), which is similar to that of WT III (−) at this pH (Figure 3). There is still, however, no proton uptake on the time-scale of the P → F formation in D132A III (−); both protons are taken up on the time scale of the F → O transition. This is essentially identical to the behavior of WT III (−) at pH 7.4 (see Figure 3 and ref *12*). Thus, at this pH, in the subunit III (−) C*c*O forms, the F → O transition is the only reaction during the single-turnover reaction that is directly linked to proton uptake through the D-pathway.

pH-Dependence of the F → O Transition (Proton Uptake) in D132A III (−). Even though at pH 7.4, the F → O transition in D132A III (−) has a rate constant similar to both WT C*c*O and WT III (−), this is largely coincidental since the pH profiles of the F → O transition of these three oxidase forms differ greatly (Figure 4). As shown here and previously (*12*), removing subunit III from WT C*c*O alters the pH-dependence of the F → O transition, such that the apparent pK_a shifts by almost two pH-units. In WT III (−) the pK_a is 6.8−7.0 (this work and ref *12*), whereas the major pH-transition in WT C*c*O (containing subunit III) shows a pK_a of 8.8 (the WT C*c*O also has a titration at lower pH (*26*)). In sharp contrast to WT C*c*O and WT III (−), the rate

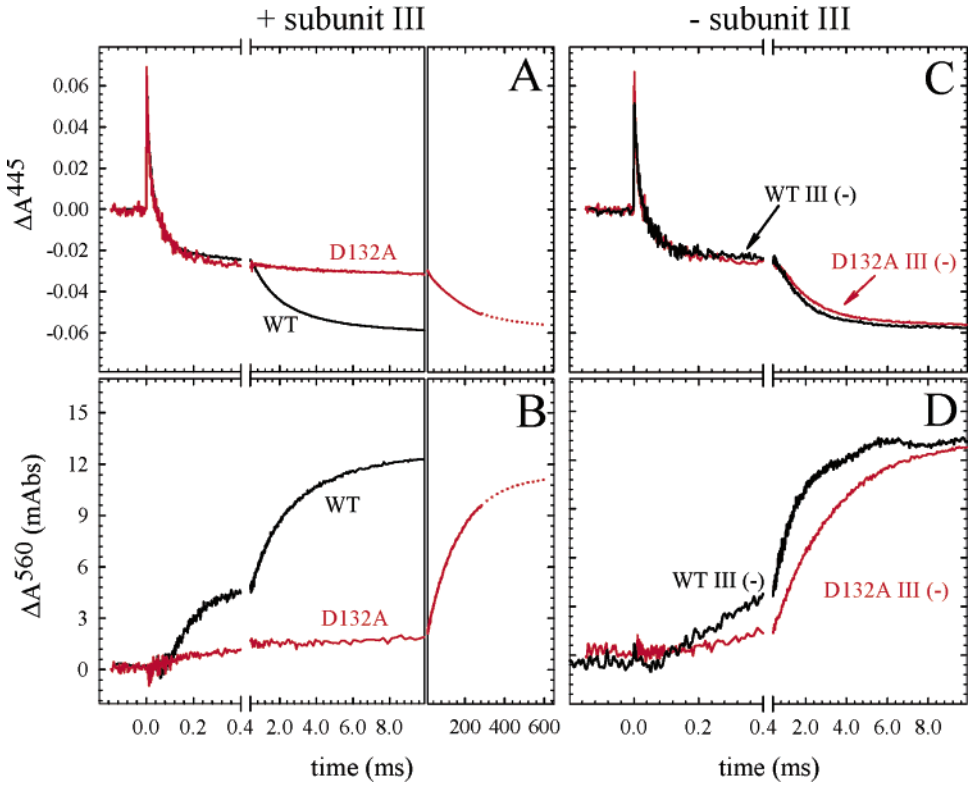

FIGURE 3: The reaction of fully reduced WT, D132A, WT III (−), and D132A III (−) C*c*Os with oxygen. Shown (A and C) are heme oxidation (at 445 nm) and proton uptake from bulk solution (B and D) in an unbuffered solution containing 40 μM of the pH-sensitive dye phenol red (λ_{max} at 560 nm). The slowest F → O transition fits to a rate constant of 800 s^{-1} in WT, 500 s^{-1} in WT III (−), 5 s^{-1} in D132A, and 300 s^{-1} in D132A III (−). In WT, after the F → O transition, there is a slower phase of uptake of a fraction of a proton with $k \sim 100$ s^{-1} (see ref *9*). In the last section of panels A and B, the fit to $k = 5$ s^{-1} for D132A is shown as a dashed extension of the experimental traces to indicate the final level. Experimental conditions: 50 mM KCl (20 mM Hepes), 0.05% DDM, 1 μM reacting C*c*O, pH ~7.4. In the traces shown at 560 nm, the small residual absorbance changes due to electron transfer in C*c*O observed in the presence of buffer have been subtracted from the unbuffered traces. See text for details.

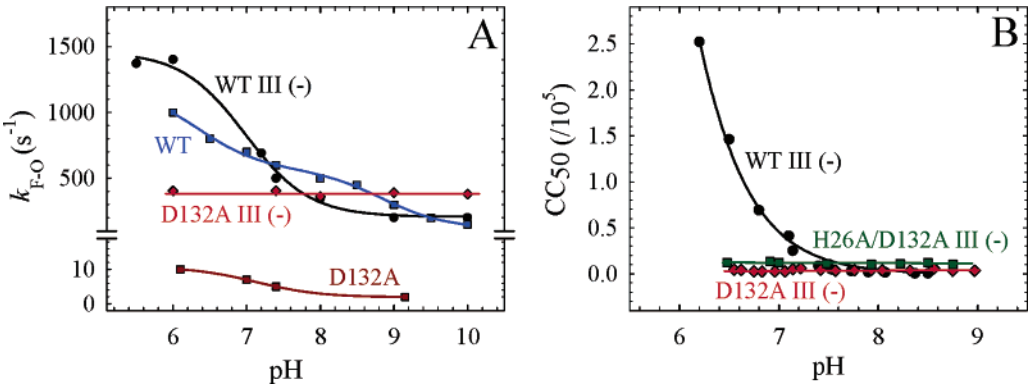

FIGURE 4: (A) pH profiles of the F → O transition rate constant in D132A III (−) (red diamonds) compared to WT III (−) (black circles). Also shown is the pH-dependence in WT (blue squares) and D132A (dark red squares). Note that in D132A III (−) the transition is independent of pH in the range from 6 to 10 in contrast to the WT III (−). Fitted pK_a's are WT III (−): pK_a = 7.0, WT: pK_a(2) = 8.8 (and pK_a(1) = 6.3, see text). The WT data are from ref *26*, and some WT III (−) data points from ref *12*. The data for D132A were tentatively fitted to a pK_a = 7.0. Experimental conditions as in Figure 3 but with 100 mM of different buffers as described in the text. (B) pH profiles of the catalytic life span (CC_{50}) of WT III (−) (black circles), D132A III (−) (red diamonds), and H26A−D132A III (−) (green squares). Catalytic life span, which reflects steady-state proton uptake by the D-pathway, was measured during cytochrome *c*-driven O_2 reduction as explained in Materials and Methods and in ref *8*.

constant for the F → O transition of D132A III (−) is unaltered from pH 6−10 (Figure 4).[2]

Thus, the rate of proton uptake through the D-pathway of D132A III (−) is unchanged from pH 6−10, while WT C*c*O and WT III (−) show large changes in the rate of proton uptake in this pH range (Figure 4).

In D132A containing subunit III, the very slow F → O transition rate constant (~5 s^{-1} at pH 7.5) is pH-dependent (Figure 4A) and could be fitted with a tentative pK_a ~ 7.0. However, due to practical reasons such as rereduction by the ascorbate/PMS system on the time-scale of the very slow F → O transition, this pK_a should be considered approximate.

[2] The rate constant for the F → O transition in D132A III (−) varied between preparations from ~300 to ~400 s^{-1}. However, within each preparation, the observed rate constant was always pH-independent.

Measurements of the Catalytic Life Span of CcO Reveal the pH Dependence of Proton Uptake during Steady-State Turnover. Recently, it was shown that the catalytic life span of C*c*O depends on the rate of proton transfer to the active site via the D-pathway (*8*). Slow proton uptake through the D-pathway leads to suicide inactivation as a result of spontaneous structural alterations at the heme a_3−Cu_B active site (*7*), and the probability of suicide inactivation increases as the rate of proton uptake decreases (*8*). The measure of catalytic life span is the CC_{50}, which is the average number of catalytic cycles (one CC = $1O_2 \rightarrow 2H_2O$) each oxidase monomer performs before it inactivates (*8*). Measurement of the CC_{50} vs pH for WT III (−) initially shows the same pH dependence as the F → O transition (Figure 4A,B), but the catalytic life span continues to increase as pH declines (see Discussion). Measurement of the CC_{50} vs pH for D132A III (−) shows the same pH independence as measurements of the F → O rate constant vs pH (Figure 4A,B). Since the catalytic lifetime is measured during steady-state O_2 reduction, the CC_{50} measurements indicate that steady-state proton uptake by D132A III (−) and WT III (−) responds to pH in the same manner as proton uptake in the single turnover experiments. Even though a greater CC_{50}, or catalytic life span, indicates more rapid proton uptake through the D-pathway, considerably more data will be required to firmly establish the relationship between the CC_{50} and the rate constants of proton uptake.

His-26, the close neighbor of Asp-132 (Figure 8) has previously been proposed as the likely alternative proton donor/acceptor for the D-pathway in the absence of Asp-132 and subunit III (*15*). To test this, the double mutant H26A−D132A was created, and subunit III was removed. The O_2 reduction activity of H26A−D132A III (−) (V_{max} = 790 s^{-1} at pH 6.5) is greater than that of D132A III (−) (V_{max} = 520 s^{-1}), while the pH dependence of steady-state proton uptake by H26A−D132A III (−), from catalytic life span determinations, is the same as D132A III (−) (see Figure 4B). These results eliminate His-26 as the alternative proton donor/acceptor (see Discussion).

Effects of Arachidonic Acid on Proton Uptake through the D-Pathway in WT III (−) and D132A III (−) CcOs. Aa, a long-chain unsaturated fatty acid, has been shown to stimulate turnover activities in mutants where Asp-132 has been exchanged for nonprotonatable amino acids (*15*, *23*, *24*). The carboxylate group of Aa is thought to substitute for the missing carboxylate of Asp-132 (*24*). The turnover activity of D132A III (−), already higher than that of D132A containing subunit III, is further stimulated about 2-fold by Aa at pH 7.4 (*8*). In this study, we investigated if the Aa-dependent increase in turnover activity is indeed due to a further increase in the rate of proton uptake through the D-pathway. The results, presented in Figure 5 clearly show a 3-fold increase (from ∼300 to ∼900 s^{-1}) in the rate constant of the F → O transition and the coupled proton uptake at pH 7.3 in D132A III (−) in the presence of 250 μM Aa. The more striking find is that Aa alters the pH dependence of proton uptake through the D-pathway completely (Figure 6A,B). While the rate constant for the F → O transition is pH independent between pH 6 and 10 in D132A III (−) without Aa, the fatty acid restores pH dependence in this range, yielding a pK_a = 7.6 (Figure 6B).

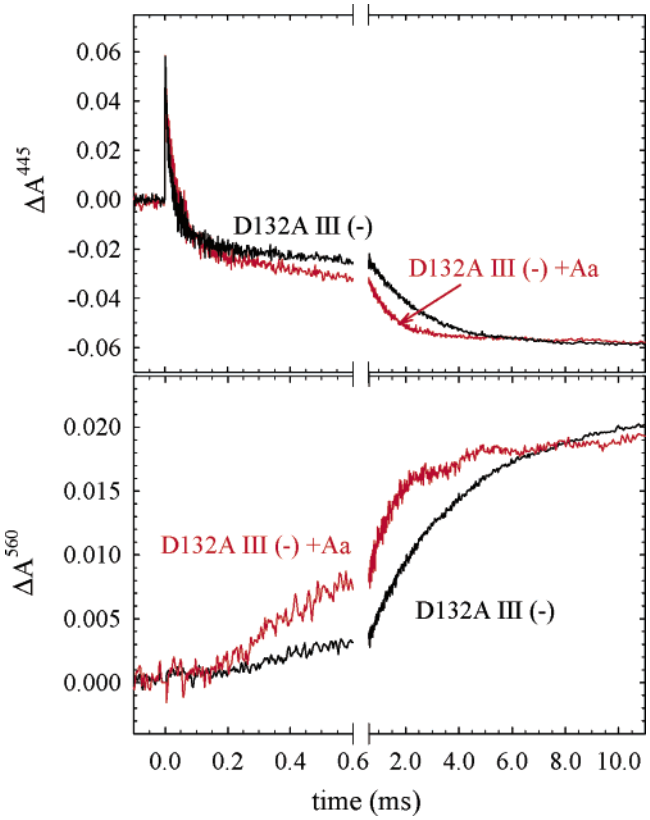

FIGURE 5: Proton uptake during the reaction of fully reduced D132A III (−) with oxygen in the presence and in the absence of 250 μM arachidonic acid (Aa). Upper panel: 445 nm, showing oxidation of hemes *a* and a_3. Lower panel: Proton uptake from solution measured using phenol red at 560 nm. Experimental conditions as in Figure 3. The rate constants for the F → O transition and the coupled proton uptake were 300 s^{-1} in the absence and 900 s^{-1} in the presence of A, respectively. The amplitude of the absorbance change at 560 nm in the presence of A was ∼3 times smaller (due to the buffering capacity of Aa) and has been scaled to the absorbance change in the absence of Aa.

In WT III (−), it was previously shown that Aa shifts the apparent pK_a of the rate of steady-state O_2 reduction from ∼7.0 to ∼7.8, but at pH 7.3 the rates of O_2 reduction in the presence and in the absence of Aa are nearly the same (*8*). Direct proton uptake measurements closely reflect this pattern of WT III (−) turnover activity; no significant changes were observed in the rate of proton uptake rate at pH ∼7.3 (data not shown), but the pK_a for the F → O transition shifts from 7.0 to 7.6 in the presence of Aa (Figure 6A).

Thus, in the presence of Aa, the apparent pK_a for proton transfer through the D-pathway becomes the same for both WT III (−) and D132A III (−) (Figure 6A,B). The same is true for the apparent pK_a's of turnover O_2 reduction by these two oxidase forms in the presence of Aa (*8*).

For both WT III (−) and D132A III (−), the changes in catalytic life span (CC_{50}) with pH in the presence of Aa show the same pattern as the pH dependence of the rate constant of the F → O transition (Figure 6C,D). This further confirms that catalytic life span reflects the rate of proton uptake through the D-pathway (*8*), and it demonstrates that Aa is having the same effect on proton uptake into the D-pathway during steady-state turnover as it does during the single turnover of the enzyme.

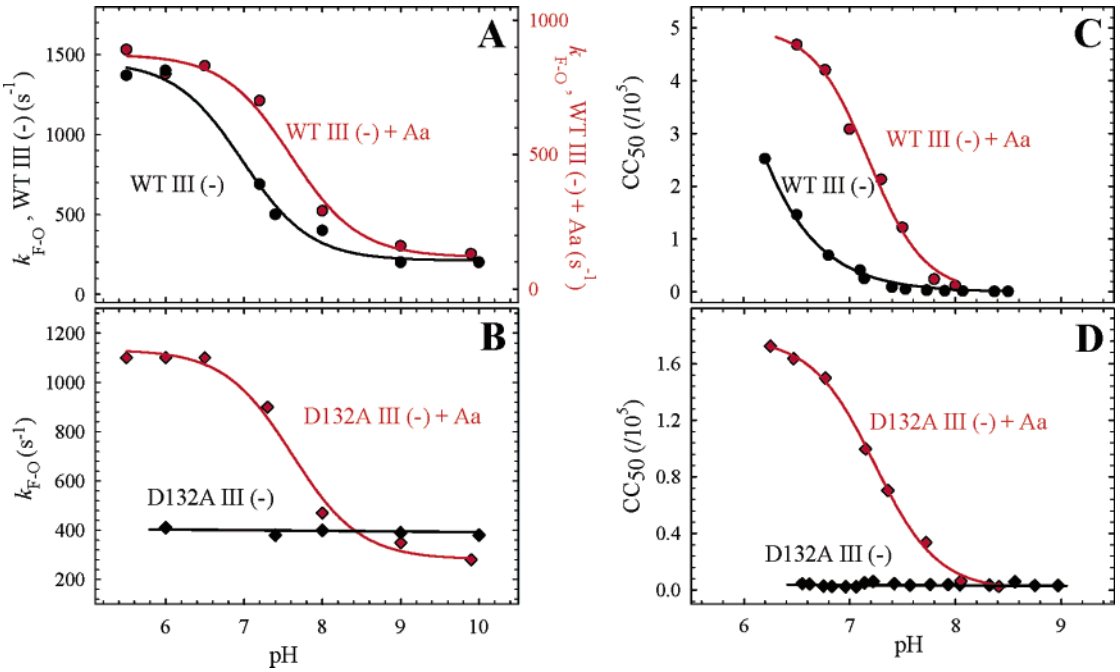

FIGURE 6: (A,B) pH profiles of the F → O transition in the absence and in the presence of 250 μM A. The pK_a's obtained from the fits are WT III (−) pK_a = 7.0, WT III (−) + Aa: pK_a = 7.6, D132A III (−) + Aa, pK_a = 7.6. Note that in the upper panel, to emphasize the difference in the pK_a, the *y*-axes for WT III (−) and WT III (−) + Aa are different. Note also that in the presence of Aa, the apparent pK_a's in WT III (−) D132A III (−) are identical (7.6). (C,D) pH profiles of catalytic life span (CC_{50}) of WT III (−) and D132A III (−) in the presence (red) and in the absence (black) of 250 μM Aa. Other conditions were as in Figure 4B.

DISCUSSION

The pH-Dependence of Proton Uptake Rates (F → O Transition) Reflects the pK_a of the Surface Donor for the D-Pathway in CcOs Lacking Subunit III. The transition that precedes F → O, the P → F transition, involves no electron transfer into the active site, but it is coupled to proton uptake from the bulk solution in WT C*c*O ($k \sim 10^4$ s^{-1} at pH 7.5). The pH titration of the rate constant for this transition in WT yields a pK_a of 9.4, which has been attributed to Glu-286 (*27*). The P → F transition was modeled as a reaction limited by the rate of proton transfer from Glu-286 to the P intermediate, followed by much faster proton uptake through the D-pathway from bulk solution to reprotonate Glu-286 (*23*, *27*). In the following transition, F → O, the same reactions occur, i.e., proton uptake through the D-pathway to Glu-286 and onto the F intermediate (see Figure 2). In the F → O reaction, electron transfer into the active site must also occur (see Figure 2), making the F → O transition much slower (~10^3 s^{-1} at pH 7.5) than the P → F transition. The reduction of F is fast, but, unlike P, reduced but deprotonated F is unstable, and therefore, it does not accumulate (*26*). This slows the F → O transition because at any time only a small fraction of F is reduced and ready to accept a proton (see ref *26* for a detailed explanation). In analogy with the P → F transition, the high pK_a of the F → O transition (pK_a ~ 8.6 in WT C*c*O) has been attributed to Glu-286. The rate constant for F → O is thus also (partly) limited by the internal transfer of a proton from Glu-286 to the binuclear site, followed by more rapid reprotonation from bulk through the D-pathway.

Thus, in the presence of subunit III, the equilibrations of Asp-132 with bulk and Glu-286 with Asp-132 are fast enough so that the observed rate constant of the F → O transition only reflects the rate constant for internal proton transfer from Glu-286 to the F intermediate times the fraction of protonated Glu-286.

In WT III (−), however, no rapid proton uptake occurs on the time-scale of the P → F transition at physiological pH (this work and ref *12*). This indicates that in the absence of subunit III the F → O transition is primarily rate-limited by the actual uptake of protons into the D-pathway, i.e., proton transfer from the surface donor to Glu-286 now limits the F → O transition. In comparison, the transfer from Glu-286 to F is fast.

Given this situation, the pH-profiles for subunit III-depleted C*c*Os no longer reflect the pK_a of Glu-286 but instead approximate the pK_a of the proton donor at the protein surface, presumed to be Asp-132 in the case of WT III (−). In support of this, the pK_a for the F → O transition of subunit III-depleted WT C*c*O is shifted dramatically when Asp-132 is altered to alanine. The pK_a of the donor to the D-pathway in D132A III (−) could not be determined, but it must lie outside the measurable range, i.e., >10, or below 5 (see Figure 4). The fact that the rate constant observed in the pH range 5−10 is quite high (and essentially the same as the turnover V_{max}) argues strongly for a pK_a > 10, since a deprotonated donor would presumably not support a high rate of proton uptake (see below for detailed discussion on the proton donor in D132A III (−)).

At pH 7.5 and lower, in both WT III (−) and D132A III (−), the rate constants observed for proton uptake into the D-pathway are slow enough to be accounted for by proton transfer directly from bulk. However, we consider it more accurate to view the reaction as limited by transfer from the surface donor into the pathway and not by the transfer of a proton through bulk water to the initial donor for two reasons. First, the pH-dependence for a rate constant of proton uptake that is limited by the rate of proton transfer from the bulk

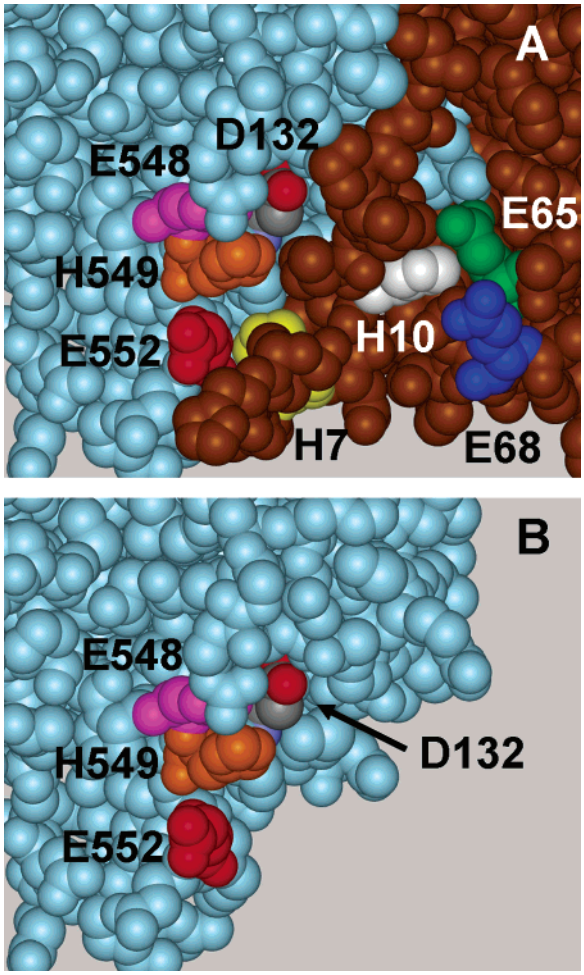

FIGURE 7: Asp-132 on the inner surface of C*c*O at an interface of subunit I (light blue) and subunit III (brown). The image, prepared using WebLab ViewerPro (Molecular Simulations) from the crystal structure of the four-subunit aa_3-type *R. sphaeroides* oxidase (PDB ID 1M56, (*35*)) shows a region of the inner (cytoplasmic) surface of the protein with the atoms in the space-filling format. Asp-132 is shown in elemental colors; one of its carboxylate oxygens protrudes and one is buried. (A) Potential participants of the surface proton antenna within 15 Å of Asp-132 are colored, including Glu-548 (pink), His-549 (orange), and Glu-552 (red) of subunit I and His-7 (yellow), His-10 (white), Glu-65 (green), and Glu-68 (blue) of subunit III. (B) Subunit III is removed, showing the loss of putative antenna residues and the potential for increased access of bulk water to Asp-132.

phase should not saturate at lower pH. Second, at higher pH, the observed rate constants become too great to be accounted for by bulk diffusion. For example, at pH 10, the F → O rate constants are 200 and 400 s^{-1} in WT III (−) and D132A III (−), respectively. These values yield apparent diffusion constants of $2-4 \times 10^{12}$ M^{-1} s^{-1}, significantly greater than the rate constant of 4×10^{10} M^{-1} s^{-1} for proton diffusion through water (*28*). This suggests that the equilibrations between Asp-132 (or an alternative donor) with the bulk is assisted by a proton-collecting antenna that persists even in the absence of subunit III (see below).

The reason the proton-transfer rate from Asp-132 into the D-pathway becomes much slower in the absence of subunit III is not fully understood yet but could be due to a decline in its pK_a (ref *12* and see below) or in its conformation due to loss of the interactions made with nearby residues on subunit III.

Measurements of CcO Catalytic Life Span Reflect the Activity of the D-Pathway during Steady-State Turnover. Slow proton uptake by the D-pathway, but not the K-pathway, induces suicide inactivation of C*c*O, especially in the absence of subunit III but also in subunit III-containing D-pathway mutations that slow proton transfer to the active site (*8*). Extended lifetimes of the reactive oxoferryl intermediates P and F occur as a result of slow proton uptake through the D-pathway, either as a result of inhibiting mutations or from decreasing pH, which increases the probability of irreversible, destructive chemistry in the active site of C*c*O during any given catalytic cycle (*7*, *8*). Thus, the catalytic life span of C*c*O decreases as the rate of proton uptake via the D-pathway decreases (*8*).

Figures 4 and 6 show that the pH dependencies of the catalytic life spans of WT III (−) and D132A III (−) are similar to the pH dependencies of the rate constants of proton uptake measured for these oxidase forms in the single turnover experiments. This is consistent with previous results (*8*) and shows that, for D-pathway mutants, measurements of catalytic life span can be used to assess relative changes in the rate and pH-dependence of proton flow to the active site via the D-pathway. Moreover, catalytic life span reflects proton flow in the steady state, an important complement to the single turnover measurements. As of yet, there is insufficient data to reliably convert CC_{50} values into actual rates of proton transfer. As seen in Figure 4, the catalytic life span of WT III (−) titrates in the same pH region as the rate constant for the F → O transition but does not show saturation at lower pH. This behavior could be related to a partial return of the rapid P → F proton uptake (as observed previously at pH 5.5 (*12*)), which may help to protect the heme a_3−Cu_B site against inactivation.

It should be noted that catalytic life span measurements yield information about steady-state proton uptake that is not obvious from measurements of the rates of steady-state O_2 reduction. For example, the initial rate of steady-state O_2 reduction by D132A III (−) declines to low levels by pH 9, with an apparent pK_a of 8.1 (*15*). The catalytic life span, however, remains constant, indicating that the rate of proton uptake into the D-pathway is unaltered (Figure 4B). It seems likely that the rate of proton uptake via the K-pathway controls the rate of steady-state O_2 reduction by D132A III (−) at high pH. Catalytic life span measurements report the steady-state activity of the D-pathway; the CC_{50} is unaffected by the rate of proton uptake via the K-pathway (*8*).

Characterization of D132A. The low turnover activity, loss of pumping capability (*13*), and slow uptake of substrate protons (*23*) in C*c*Os where Asp-132 is exchanged for nonprotonatable amino acids are well-known and have led to important insights into the catalytic mechanism. Asp-132 sits at the entrance to the D-pathway and donates protons to a chain of waters that leads to the other crucial residue in the pathway, Glu-286, which is located 26 Å above Asp-132 and ~10 Å from Cu_B. A key difference between C*c*Os lacking Asp-132 and those lacking Glu-286, is that in the Glu-286 mutant C*c*Os, the flow-flash reaction effectively stops at intermediate P (*29*, *30*), while Asp-132 mutants, such as D132N (*23*), go on to form intermediate F. The formation of intermediate F requires proton transfer to the active site (Figure 2) (*23*). Since no proton uptake from bulk solution

takes place on the time-scale of the P → F transition in D132N, the proton used to form F is abstracted internally, apparently from Glu-286. In the single turnover experiments presented here, we show that D132A containing subunit III behaves the same as D132N of *R. sphaeroides*, i.e., severe inhibition of the rate of proton uptake (Figure 3) and the rapid formation of F by the movement of an internal proton to the heme a_3−Cu_B site.

When subunit III is removed from D132A, the rate of proton uptake through the D-pathway *increases* by almost 2 orders of magnitude, from the very slow 5 to ∼400 s^{-1} (see Figure 3). This finding explains the parallel increase in O_2 reduction activity previously observed upon the removal of subunit III from D132A (*15*). There is still, however, no rapid proton uptake on the time-scale of the P → F transition, as occurs in WT C*c*O.

The increase in the proton uptake rate upon the removal of subunit III from D132A indicates that in the absence of subunit III, the structure of the protein around position 132 "opens up" for proton transfer into the D-pathway, which now has no absolute requirement for Asp-132. The identity of the proton donor/acceptor that substitutes for Asp-132 is discussed below. An alternative, that the removal of subunit III increases proton uptake from the outer surface of D132A, rather than by its D-pathway, can be ruled out. The removal of subunit III inhibits proton backflow (*14*). Further, the removal of subunit III from D132A restores the normal stimulation of activity in C*c*O-vesicles by uncouplers, a hallmark of proton uptake from the inner surface (*14*).

Role of Subunit III and the Area around Asp-132 for Proton Uptake into the D-Pathway. In WT C*c*O including subunit III, proton uptake occurs at 10^4 s^{-1} (the rate constant for the P → F transition) up to pH ∼ 9. The calculated bimolecular rate constant for proton uptake at this pH (k·1/[H^+]) is thus 10^{13} M^{-1} s^{-1} (*27*). This value far exceeds that allowed by diffusion of protons to the initial proton donor through bulk water (4×10^{10} M^{-1} s^{-1}) and provides evidence for the presence of a "proton antenna" (see e.g., ref *31*). An antenna for the D-pathway has been proposed to use surface-exposed residues to attract and transfer protons along the protein surface to speed reprotonation of the initial proton donor (*32*). Several residues within 15 Å of Asp-132 are well positioned to function as a proton antenna (Figure 7). The disappearance of rapid (10^4 s^{-1}) proton uptake in WT III (−) and D132A III (−) at physiologic pH values could be due to the loss of the subunit III portion of the proton antenna (*12*). However, as noted above, the apparent diffusion constants of $2-4 \times 10^{12}$ M^{-1} s^{-1} achieved by WT III (−) and D132A III (−) for proton uptake during the F → O transition at high pH suggest the presence of a functional, but less effective, proton antenna in the absence of subunit III. Thus, a proton antenna independent of subunit III must be presumed to be functional at physiologic pH even though the rates of proton uptake observed in this pH range could be achieved by the diffusion of protons through water directly to the initial proton donor/acceptor of the D-pathway.

For the WT enzyme, the removal of subunit III should leave Asp-132 and surrounding residues more exposed to water. In fact, an analysis of the WT C*c*O of *R. sphaeroides* in the absence of subunit III shows waters around Asp-132 that would otherwise be occluded by subunit III (*33*). On the basis of the pH dependence of the F → O transition, the pK_a of Asp-132 in WT III (−) appears to be ∼7. The pK_a of Asp-132 in the presence of subunit III is not known, but since the carboxylate group is more sheltered from bulk water in the presence of subunit III, the carboxylate anion will be less stable and the pK_a of Asp-132 is likely to be higher. A decreased pK_a of Asp-132 in the absence of subunit III could thus be part of the reason the rate constant for proton uptake is lowered at pH 7.5 (suggested also in ref *12*), since with a pK_a of 7 Asp-132 would only be partly protonated at this pH.

When Asp-132 is altered to alanine in C*c*O containing subunit III, the D-pathway is extremely inhibited, with the maximum rate of proton uptake dropping from ∼10^4 to 5 s^{-1} at pH 7.4. Even with the smaller alanine side chain at position 132, the protein creates a barrier such that protons from the bulk or from the proton antenna cannot access the waters of the D-pathway. The removal of subunit III loosens this barrier, and a moderate rate of proton uptake is restored. Thus, Asp-132 in normal C*c*O is obligatory for conveying protons from bulk water and the proton antenna into the D-pathway, whereas in the absence of subunit III other donors, including water, become possible. However, the pH dependence data for WT III (−) and D132A III (−) make it clear that Asp-132, when present, is involved in transferring the protons into the pathway even in the absence of subunit III.

What Is the Proton Donor to the D-Pathway in the Subunit III-Depleted D132A Mutant CcO? The pH dependence of the F → O transition and the catalytic life span observed with D132A III (−) indicate that the alternative proton donor to the D-pathway now has a pK_a > 10. While the removal of subunit III from D132A restores activity to the D-pathway, the removal of subunit III from another D-pathway mutant, G204D, fails to do so (*34*). Since Gly-204 is located immediately above Asn-139, the next water-coordinating residue above Asp-132, the results place the location of the alternative acceptor/donor between position 132 and Asn-139. Within this region, the two groups most likely to function as an initial acceptor/donor with a pK_a above 10 are His-26, if its side chain were to cycle between the neutral imidazole and the imidazolate forms, and the first coordinated water of the D-pathway. His-26 is located immediately adjacent to Asp-132 in the normal structure, where its imidazole Nδ is 3.1 Å from the buried oxygen of the carboxylate function of Asp-132 (Figure 8). The possibility of His-26 as the pK_a > 10 donor was excluded by the finding that H26A−D132A III (−) still contains an acceptor/donor with a high pK_a. Thus, it seems likely that the initial proton acceptor/donor in D132A III (−) is the water coordinated by Asn-139. This water becomes accessible to bulk water in the absence of D132A and subunit III (Figure 8), and it may move from its position seen in the structure of WT C*c*O (*35*). In fact, a small water cluster may form, such as that recently identified as the proton release group in bacteriorhodopsin (*36*). More facile formation of a cluster in the larger pocket created by H26A−D132A III (−) could explain the increased activity of this mutant as compared to D132A III (−). It should also be noted that a recent structure of succinate dehydrogenase identifies a surface exposed water as the initial group of the proton-transfer pathway leading to the quinone binding site (*37*).

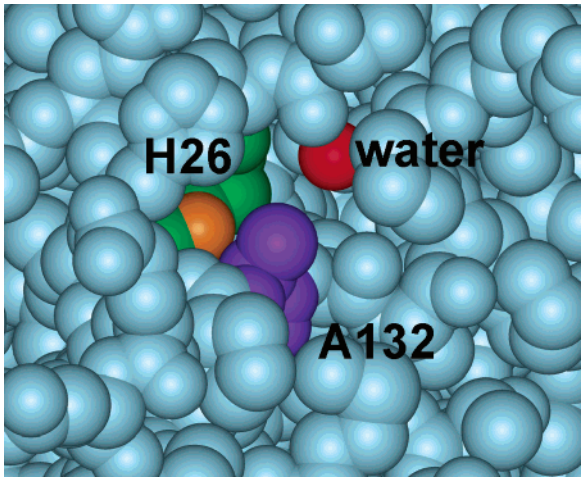

FIGURE 8: A view into the entry of the D-pathway of D132A III (−) on the inner surface of subunit I (light blue). Starting from the PDB ID 1M56 C*c*O structure (*35*), Asp-132 was mutated in silico using the program Deep View/Swiss −PdbViewer 3.7. With the conversion of Asp-132 to Ala-132 (purple), and the removal of subunit III, examination of the structure shows increased access to both His-26 (green, with its Nδ in tan) and a water coordinated by Asn-139 (the oxygen of this water is shown in red).

Arachidonic Acid Shifts the Rates and pH-Profiles of Proton Uptake into the D-Pathway. Aa, and other long chain polyunsaturated fatty acids, have previously been shown to stimulate activity in Asp-132 mutant C*c*Os (*24*), the increase being due to a more efficient proton transfer into the D-pathway (*23*). This increase has been suggested to be due to the carboxylate group of the Aa being able to substitute as the proton donor into the D-pathway in the absence of Asp-132, i.e., partial chemical rescue. Aa also stimulates the steady-state O_2 reduction activity of D132A III (−) and WT III (−) but not WT C*c*O (*15*, *24*). The addition of Aa elicits a striking change for D-pathway proton uptake in D132A III (−), a 3-fold increase in the rate of proton uptake at pH 7.3 and a shift in the pK_a of the F → O transition from >10 to 7.6. Steady-state proton uptake, via catalytic life span measurements, shows a similar response. These results indicate a change in the identity of the initial proton donor for the D-pathway, presumably to Aa itself. In support of this, the pK_a values of the F → O transition and steady-state proton uptake of WT III (−) as well as D132A III (−) become exactly the same once Aa is added. The results strongly suggest that Aa becomes the initial proton donor for the D-pathway for both of these oxidase forms, which otherwise are enormously different. The close pK_a values further suggest that the carboxylate group of Aa is bound in the same position in either the presence or the absence of Asp-132. Aa also stimulates the activity of G204D (*34*), suggesting that the headgroup of the fatty acid can access a water of the D-pathway some 13 Å above Asp-132. In the absence of subunit III, a binding site on the exposed surface of subunit I that is normally covered by subunit III may allow such access since the waters of the D-pathway are close to this surface. The fact that Asp-132 and Aa are both molecules with a carboxylate group may explain why the pK_a of proton uptake by WT III (−) is less altered by Aa than the estimated pK_a of D132A III (−).

These results are qualitatively similar to the effects of Aa on the steady-state O_2 reduction activity of D132A III (−) and WT III (−) and thus confirm the earlier hypothesis that the changes in turnover were due to changes in the D-pathway activity (*15*).

Proton Pumping. Protons destined for the proton pump of C*c*O are taken up exclusively through the D-pathway. Despite its slower rate of D-pathway proton uptake at pH 7.4, WT III (−) retains proton pumping capability at this pH, albeit with lower stoichiometry than WT C*c*O containing subunit III (*15*). The D132A mutant was one of the first shown to have its residual O_2-reducing capability uncoupled from proton pumping, as measured in the standard multiple-turnover pumping assay (*13*). After the removal of subunit III from D132A, the rate of D-pathway proton uptake at pH 7.4 is similar to that of WT III (−), but proton pumping is not regained (*15*). On the basis of our results, this failure to pump protons is likely related to the shift in the pK_a of the initial proton donor. Fine-tuning of the pK_a's of amino acid residues involved in the pumping machinery, especially Glu-286, has been shown to be important (*38*, *39*) to protonate/deprotonate the different components of the pumping machinery in the "right" sequence in time. In the case of D132A III (−), the lack of proton pumping is likely because the pK_a of the initial donor (suggested to be a water molecule) is low enough to donate protons to the O_2 reduction intermediates (e.g., F) but too high to populate the protonated states of the other components of the pumping machinery, including Glu-286.

Since Aa provides a low pK_a proton donor for the D-pathway, proton pumping should presumably be regained. Unfortunately, pumping cannot be measured in the presence of Aa, because of the uncoupling effects of the fatty acid (*24*).

CONCLUSIONS

Analysis of the kinetics of proton uptake into the D-pathway indicates that in the absence of subunit III the transfer of the proton from Asp-132 to the waters of the pathway is the likely rate-limiting step. In the absence of subunit III, the pK_a of Asp-132 is ~7, and this value may increase in the presence of subunit III since Asp-132 will have less interaction with bulk water. In the absence of subunit III and Asp-132, a water of the D-pathway becomes the initial proton donor/acceptor, rather than a nearby histidine residue. In the absence of subunit III, the carboxylate group of Aa may function as the initial proton donor/acceptor whether or not Asp-132 is present. Thus, two functions of subunit III have been clarified; subunit III facilitates the transfer of protons from Asp-132 into the D-pathway and subunit III provides part of a structural barrier that prevents alternative proton donors from gaining access to the waters of the D-pathway.

ACKNOWLEDGMENT

We would like to thank Peter Brzezinski (Stockholm University) for stimulating discussions and Jimmy Gray and Anna Murphree (University of Mississippi Medical Center) for technical expertise.

REFERENCES

1. Brzezinski, P. (2004) Redox-driven membrane-bound proton pumps, *Trends Biochem. Sci. 29*, 380−387.

2. Ferguson-Miller, S., and Babcock, G. T. (1996) Heme-copper terminal oxidases, *Chem. Rev. 96*, 2889−2907.
3. Wikström, M. (2004) Cytochrome *c* oxidase: 25 years of the elusive proton pump, *Biochim. Biophys. Acta 1655*, 241−247.
4. Saraste, M. (1999) Oxidative phosphorylation at the fin de siecle, *Science 283*, 1488−1493.
5. Calhoun, M. W., Thomas, J. W., and Gennis, R. B. (1994) The cytochrome oxidase superfamily of redox-driven proton pumps, *Trends Biochem. Sci. 19*, 325−330.
6. Bratton, M. R., Hiser, L., Antholine, W. E., Hoganson, C., and Hosler, J. P. (2000) Identification of the structural subunits required for formation of the metal centers in subunit I of cytochrome *c* oxidase of *Rhodobacter sphaeroides*, *Biochemistry 39*, 12989−12995.
7. Bratton, M. R., Pressler, M. A., and Hosler, J. P. (1999) Suicide inactivation of cytochrome *c* oxidase: catalytic turnover in the absence of subunit III alters the active site, *Biochemistry 38*, 16236−16245.
8. Mills, D. A., and Hosler, J. P. (2005) Slow proton transfer through the pathways for pumped protons in cytochrome *c* oxidase induces suicide inactivation of the enzyme, *Biochemistry 44*, 4656−4666.
9. Ädelroth, P., Ek, M., and Brzezinski, P. (1998) Factors determining electron-transfer rates in cytochrome *c* oxidase: investigation of the oxygen reaction in the *R. sphaeroides* enzyme, *Biochim. Biophys. Acta 1367*, 107−117.
10. Babcock, G. T. (1999) How oxygen is activated and reduced in respiration, *Proc. Natl. Acad. Sci. U.S.A.* 96, 12971−12973.
11. Blomberg, M. R., Siegbahn, P. E., Babcock, G. T., and Wikström, M. (2000) O−O bond splitting mechanism in cytochrome oxidase, *J. Inorg. Biochem. 80*, 261−269.
12. Gilderson, G., Salomonsson, L., Aagaard, A., Gray, J., Brzezinski, P., and Hosler, J. (2003) Subunit III of cytochrome *c* oxidase of *Rhodobacter sphaeroides* is required to maintain rapid proton uptake through the D pathway at physiologic pH, *Biochemistry 42*, 7400−7409.
13. Fetter, J. R., Qian, J., Shapleigh, J., Thomas, J. W., Garcia-Horsman, A., Schmidt, E., Hosler, J., Babcock, G. T., Gennis, R. B., and Ferguson-Miller, S. (1995) Possible proton relay pathways in cytochrome *c* oxidase, *Proc. Natl. Acad. Sci. U.S.A. 92*, 1604−1608.
14. Mills, D. A., and Ferguson-Miller, S. (2003) Understanding the mechanism of proton movement linked to oxygen reduction in cytochrome *c* oxidase: lessons from other proteins, *FEBS Lett. 545*, 47−51.
15. Mills, D. A., Tan, Z., Ferguson-Miller, S., and Hosler, J. (2003) A role for subunit III in proton uptake into the D pathway and a possible proton exit pathway in *Rhodobacter sphaeroides* cytochrome *c* oxidase, *Biochemistry 42*, 7410−7417.
16. Zhen, Y., Qian, J., Follmann, K., Hayward, T., Nilsson, T., Dahn, M., Hilmi, Y., Hamer, A. G., Hosler, J. P., and Ferguson-Miller, S. (1998) Overexpression and purification of cytochrome *c* oxidase from *Rhodobacter sphaeroides*, *Protein Expr. Purif. 13*, 326−336.
17. Keen, N. T., Tamaki, S., Kobayashi, D., and Trollinger, D. (1988) Improved broad-host-range plasmids for DNA cloning in gram-negative bacteria, *Gene 70*, 191−197.
18. Cao, J., Hosler, J., Shapleigh, J., Revzin, A., and Ferguson-Miller, S. (1992) Cytochrome aa3 of *Rhodobacter sphaeroides* as a model for mitochondrial cytochrome *c* oxidase. The coxII/coxIII operon codes for structural and assembly proteins homologous to those in yeast, *J. Biol. Chem. 267*, 24273−24278.
19. Hiser, L., Di Valentin, M., Hamer, A. G., and Hosler, J. P. (2000) Cox11p is required for stable formation of the Cu(B) and magnesium centers of cytochrome *c* oxidase, *J. Biol. Chem. 275*, 619−623.
20. Shapleigh, J. P., and Gennis, R. B. (1992) Cloning, sequencing and deletion from the chromosome of the gene encoding subunit I of the aa3-type cytochrome *c* oxidase of *Rhodobacter sphaeroides*, *Mol. Microbiol. 6*, 635−642.
21. Kovach, M. E., Elzer, P. H., Hill, D. S., Robertson, G. T., Farris, M. A., Roop, R. M., 2nd, and Peterson, K. M. (1995) Four new derivatives of the broad-host-range cloning vector pBBR1MCS, carrying different antibiotic-resistance cassettes, *Gene 166*, 175−176.
22. Brändén, M., Sigurdson, H., Namslauer, A., Gennis, R. B., Ädelroth, P., and Brzezinski, P. (2001) On the role of the K-proton-transfer pathway in cytochrome *c* oxidase, *Proc. Natl. Acad. Sci. U.S.A. 98*, 5013−5018.
23. Smirnova, I. A., Ädelroth, P., Gennis, R. B., and Brzezinski, P. (1999) Aspartate-132 in cytochrome *c* oxidase from *Rhodobacter sphaeroides* is involved in a two-step proton transfer during oxo-ferryl formation, *Biochemistry 38*, 6826−6833.
24. Fetter, J., Sharpe, M., Qian, J., Mills, D., Ferguson-Miller, S., and Nicholls, P. (1996) Fatty acids stimulate activity and restore respiratory control in a proton channel mutant of cytochrome *c* oxidase, *FEBS Lett. 393*, 155−160.
25. Mills, D. A., Schmidt, B., Hiser, C., Westley, E., and Ferguson-Miller, S. (2002) Membrane potential-controlled inhibition of cytochrome *c* oxidase by zinc, *J. Biol. Chem. 277*, 14894−14901.
26. Brändén, G., Brändén, M., Schmidt, B., Mills, D. A., Ferguson-Miller, S., and Brzezinski, P. (2005) The protonation state of a heme propionate controls electron transfer in cytochrome C oxidase, *Biochemistry 44*, 10466−10474.
27. Namslauer, A., Aagaard, A., Katsonouri, A., and Brzezinski, P. (2003) Intramolecular proton-transfer reactions in a membrane-bound proton pump: the effect of pH on the peroxy to ferryl transition in cytochrome *c* oxidase, *Biochemistry 42*, 1488−1498.
28. Gutman, M., and Nachliel, E. (1990) The dynamic aspects of proton-transfer processes, *Biochim. Biophys. Acta 1015*, 391−414.
29. Ädelroth, P., Ek, M. S., Mitchell, D. M., Gennis, R. B., and Brzezinski, P. (1997) Glutamate 286 in cytochrome aa3 from *Rhodobacter sphaeroides* is involved in proton uptake during the reaction of the fully reduced enzyme with dioxygen, *Biochemistry 36*, 13824−13829.
30. Verkhovskaya, M. L., Garcia-Horsman, A., Puustinen, A., Rigaud, J. L., Morgan, J. E., Verkhovsky, M. I., and Wikström, M. (1997) Glutamic acid 286 in subunit I of cytochrome *bo*3 is involved in proton translocation, *Proc. Natl. Acad. Sci. U.S.A. 94*, 10128−10131.
31. Gutman, M., and Nachliel, E. (1995) The dynamics of proton exchange between bulk and surface groups, *Biochim. Biophys. Acta 1231*, 123−138.
32. Marantz, Y., Nachliel, E., Aagaard, A., Brzezinski, P., and Gutman, M. (1998) The proton collecting function of the inner surface of cytochrome *c* oxidase from *Rhodobacter sphaeroides*, *Proc. Natl. Acad. Sci. U.S.A. 95*, 8590−8595.
33. Cukier, R. I. (2004) Quantum molecular dynamics simulation of proton transfer in cytochrome *c* oxidase, *Biochim. Biophys. Acta 1656*, 189−202.
34. Han, D., Morgan, J. E., and Gennis, R. B. (2005) G204D, a mutation that blocks the proton-conducting D-channel of the aa3-type cytochrome *c* oxidase from *Rhodobacter sphaeroides*, *Biochemistry 44*, 12767−12774.
35. Svensson-Ek, M., Abramson, J., Larsson, G., Törnroth, S., Brzezinski, P., and Iwata, S. (2002) The X-ray crystal structures of wild-type and EQ(I-286) mutant cytochrome *c* oxidases from *Rhodobacter sphaeroides*, *J. Mol. Biol. 321*, 329−339.
36. Garczarek, F., Brown, L. S., Lanyi, J. K., and Gerwert, K. (2005) Proton binding within a membrane protein by a protonated water cluster, *Proc. Natl. Acad. Sci. U.S.A. 102*, 3633−3638.
37. Horsefield, R., Yankovskaya, V., Sexton, G., Whittingham, W., Shiomi, K., Omura, S., Byrne, B., Cecchini, G., and Iwata, S. (2006) Structural and computational analysis of the quinone-binding site of complex II (succinate-ubiquinone oxidoreductase): a mechanism of electron transfer and proton conduction during ubiquinone reduction, *J. Biol. Chem. 281*, 7309−7316.
38. Namslauer, A., Pawate, A. S., Gennis, R. B., and Brzezinski, P. (2003) Redox-coupled proton translocation in biological systems: proton shuttling in cytochrome *c* oxidase, *Proc. Natl. Acad. Sci. U.S.A. 100*, 15543−15547.
39. Brändén, G., Pawate, A. S., Gennis, R. B., and Brzezinski, P. (2006) Controlled uncoupling and recoupling of proton pumping in cytochrome *c* oxidase, *Proc. Natl. Acad. Sci. U.S.A. 103*, 317−322.
40. Humphrey, W., Dalke, A., and Schulten, K. (1996) VMD: visual molecular dynamics, *J. Mol. Graphics 14*, 33−38.

BI0605843